Salt crystallization dynamics in building rocks: a 4D study using laboratory X-ray micro-CT

H. DERLUYN*[1], M.A. BOONE[1,2], M.N. BOONE[3], T. DE KOCK[1], J. DESARNAUD[5], S. PEETERMANS[4], L. MOLARI[6], S. DE MIRANDA[6], N. SHAHIDZADEH[5], V. CNUDDE[1]

[1] UGCT – PProGRess, Dept. Geology and Soil Science, Ghent University, Krijgslaan 281/S8, B-9000 Gent, Belgium – hannelore.derluyn@ugent.be, marijn.boone@ugent.be, tim.dekock@ugent.be, veerle.cnudde@ugent.be
[2] XRE – X-ray Engineering bvba, De Pintelaan 111, B-9000 Gent, Belgium
[3] UGCT, Dept. Physics and Astronomy, Ghent University, Proeftuinstraat 86/N12, B-9000 Gent, Belgium – matthieu.boone@ugent.be
[4] NIAG, Spallation Neutron Source Division, Paul Scherrer Insitute, CH-5232 Villigen PSI, Switzerland – stevenpeetermans@gmail.com
[5] Van der Waals-Zeeman Institute, Institute of Physics, University of Amsterdam, Science Park 904, NL-1098 XH Amsterdam, The Netherlands – j.e.desarnaud@uva.nl, n.shahidzadeh@uva.nl
[6] DICAM, University of Bologna, V. le Risorgimento 2, IT-40136 Bologna, Italy – luisa.molari@unibo.it, stefano.demiranda@unibo.it
* presenting author

Keywords: building stones, 4D X-ray micro-CT, salt weathering, crystallization dynamics, drying kinetics

Abstract

We employ laboratory X-ray micro-computed tomography (µCT) during climate-controlled salt weathering experiments to acquire data on the kinetics of drying and salt precipitation and the distribution of crystals within the pore space of Mšené sandstone. For that purpose, a custom-designed setup was built at the UGCT's scanners of the Ghent University Centre for X-ray Tomography (UGCT) that allows to acquire 4D scans while drying. Samples were initially capillary saturated with a saturated NaCl-solution and subsequently dried at 20% RH and at 50% RH, at room temperature. These RH-values are representative for winter and summer conditions for the salt NaCl, which is not temperature sensitive. Different salt precipitation dynamics result in different drying kinetics at the two RH's. These crystallization and transport dynamics can be directly linked as revealed by the 4D X-ray µCT datasets.

Introduction

Salt crystallization is a major cause of weathering of building stones and cementitious materials. When saline solutions are present in these materials, the surrounding climatic conditions, i.e. temperature and humidity variations, may induce the precipitation of salts at the surface (efflorescence) or in the pore space beneath (subflorescence). During drying-induced crystallization, the distribution of salt crystals in the pore space and on the material's surface strongly influences the drying rate. Desarnaud et al. (2015) describe the effect of the crystal growth on the drying behaviour of sandstone initially saturated with NaCl solution, by comparing drying at 20% RH and 50% RH. Drying at 20% RH is found to take longer than at 50% RH, which is addressed to the formation of a salt skin on the surface at 20% RH. The drying was monitored by measuring the weight change of the sample, while the salt precipitation was characterized by SEM images and X-ray µCT after the samples had dried out. Thus, the dynamics of salt growth during evaporation was not measured up to now. Experimental data of drying and salt growth measured simultaneously would aid the advancement of the understanding of coupled drying-crystallization dynamics. This kind of data is also essential for numerical models that predict salt damage risks in building materials, as model parameters for drying as well as crystallization kinetics need to be defined.

Methods

Two cylindrical samples of 8 mm in diameter and 10 mm in height were cored from a Mšené sandstone plate. This sandstone has a unimodal pore system with an average pore size of 30 µm (Shahidzadeh-Bonn et al. 2010). The samples were initially scanned in their dry state at the X-ray µCT scanner HECTOR (Masschaele et al. 2013) of the UGCT. Next, the samples were capillary saturated by immersing them in a saturated NaCl solution for 30 minutes. The samples were then scanned in their wet state, and subsequently during their drying, by scanning them every 30 minutes during the first 3 hours, and every hour during the succeeding 12 hours. Drying was controlled by placing the sample in a custom-built climatic chamber, compatible with the µCT setup, depicted in Fig. 1. Conditioned air is produced by the GenRH-T generator (Surface Measurment Systems Ltd., UK) and blown in the plexi-glass test chamber at a slow rate (3.3 ml/s). The inner volume of the test chamber is 4x4x3 cm^3. The outlet of the chamber is connected to a separate RH-T sensor. Polyimide windows of 2x2 cm^2, which are quasi transparent to X-rays, are present at the front and the backside of the chamber. The chamber is clamped at its upper rod and has a hole in the bottom of 2 cm diameter that allows for the sample's rotation while scanning. The sample is attached to a 1 cm diameter plastic rod fixed on the rotation stage, and the flow loss was found to be minimal. This setup ensured that the samples were dried at a constant temperature of 19.2°C and a RH of 20% and 50% for the first and the second sample, respectively.

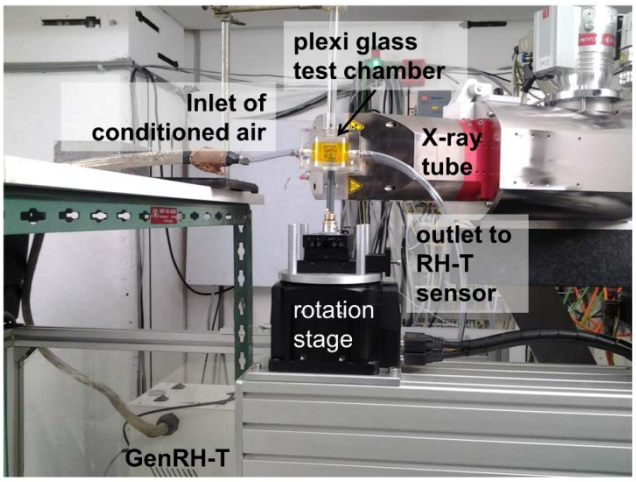

Fig. 1. *Experimental setup at the X-ray µCT scanner HECTOR of the UGCT for performing dynamic scans of salt weathering cycles.*

For each scan, a total of 1351 projections was acquired over an angle of 360°, with an exposure time of 400 ms per projection. A thin aluminum filter (1 mm) was used to block low-energetic X-rays at the source to reduce beam hardening. In order to correct for inhomogeneities of the detector and beam, 32 dark-field and 200 flat-field images were acquired before the initial scan. The X-ray tube provided a voltage of 100 kV with a target power of 10 W. The source-detector distance was 1530.7 mm and the source-object distance 38.3 mm. The projections were binned by a factor 2x2 in order to increase the signal-to-noise ratio, resulting in a reconstructed voxel size of 10^3 μm^3. The raw data were reconstructed using the software Octopus Reconstruction (Inside Matters bvba, Belgium; Vlassenbroeck et al. 2007). The same set of parameters for ring and spot removal, tilt and skew of the detector and beam hardening were adopted for all scans. Small shifts in the reconstructed volumes with respect to the reference volume were corrected by aligning all volumes to the reference scan using the software

DataViewer (SkyScan, Belgium). This ensured the same positioning in 3D space for all datasets.

The datasets were further analyzed with the software Avizo (FEI). As it was not possible to directly threshold the salt crystals and the salt solution from the image histogram, due to an overlap of the grey values of crystals and solution, the following procedure was applied: the wet scan was subtracted from the series of scans taken while drying, resulting in differential images (Boone et al. 2014), where all negative values correspond to the solution that has dried-out, and all positive values correspond to salt crystals that precipitated. Two volumes-of-interest (VOI's) were defined, one including only the sample's volume and one including the sample's volume and the salt efflorescence at the end of drying. The evolution of the volume fractions of the salt solution, the total amount of precipitated salt, the salt efflorescence and salt subflorescence were then calculated with respect to the volume of the second VOI.

Results and discussion

The drying of the two samples is given in Fig. 2a. We can observe that drying at 20% RH is initially faster than at 50% RH, due to the higher difference in RH between the sample's surface and the environment. This first drying stage is characterized by a constant rate, due to the capillary action which induces a hydraulic connection between the surface and the inner pore space. Subsequently, the evaporation at the surface mainly results in salt efflorescence. At 50% RH, this constant rate period lasts until the sample is almost completely dried out. At 20% RH, the drying changes to a slower, exponential regime after about 1 hour, i.e. after approximately half of the initial salt solution has dried out.

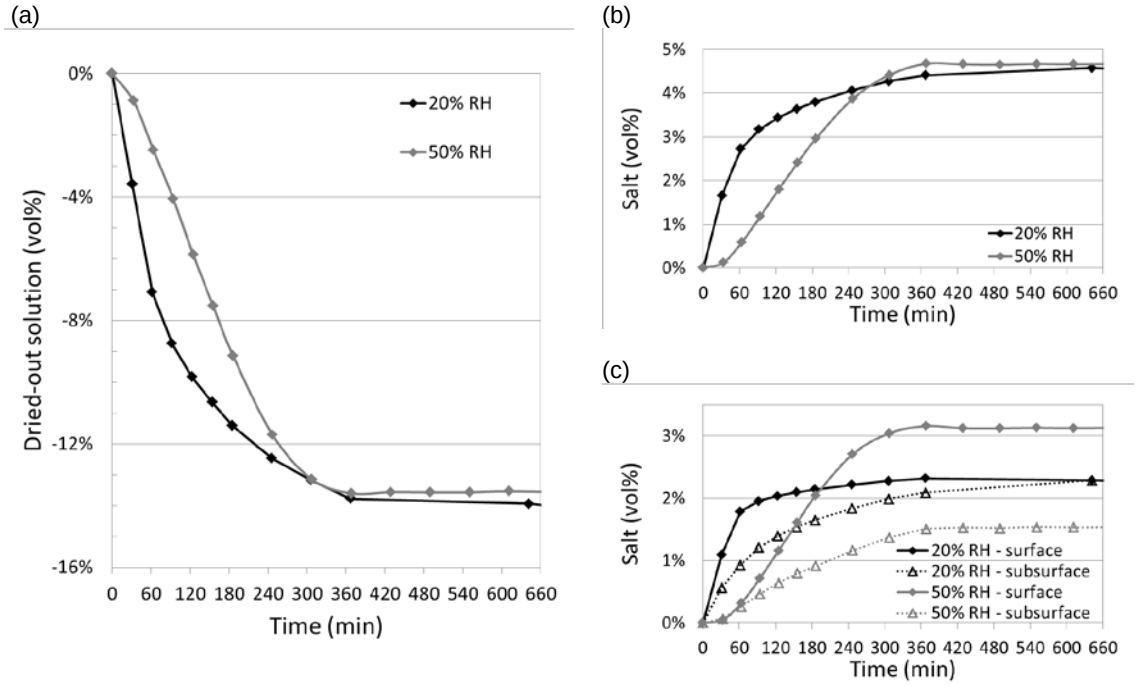

Fig. 2. *The drying (a) and crystallization dynamics (b-c) of Mšené sandstone at 20% RH and 50% RH. Fig 2c disseminates between the salt crystals forming on the outer surface (efflorescence) and the salt crystals precipitating just below, in the pores of the subsurface.*

The differences in drying kinetics are caused by the differences in salt precipitation dynamics, which are presented in Figs. 2b-c. As the initial amount of salt is equal for

both samples, the resulting total amount of salt precipitation is the same (Fig. 2b). The crystal precipitation develops however slower at 50% RH, where the salt crystals forming on the surface (efflorescence) and the salt crystals precipitating in the pores close to the surface, develop at the same relative rate during the whole duration of drying (with respect to their respective total amounts, Fig. 2c). No salt crystals were found deeper inside the volume. While drying at 20% RH, the crystal growth at the surface develops first, and much faster than at 50% RH, mainly during the first hour of the experiment and then reaches a plateau. The salt crystals precipitating just below the surface at this lower RH develop more gradually, during the whole duration of the drying. The period of the formation of efflorescence at 20% RH is congruent with the period of the constant drying rate in the drying curve. The second exponential drying stage at 20% RH must thus be resulting from this salt efflorescence, corroborating the statement that a salt skin is forming on the surface during the first stage of drying (Desarnaud et al. 2015), partially closing the pores and causing a slower drying during the continuation of the process. The salt skin still grows slightly during this second period, but most of the salt crystals precipitate just below this layer. Typical snapshots of the sample drying at 20% RH are given in Fig. 3.

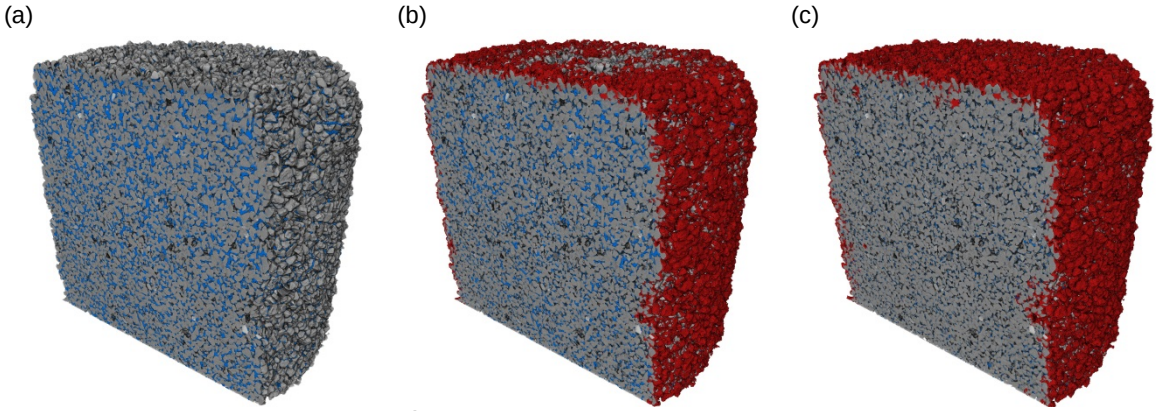

Fig. 3. *Typical snapshots of the Mšené sandstone sample while drying at 20% RH at the wet state (a), after 1 hour (b) and after 6 hours (c). Blue: salt solution – red: salt crystals.*

Acknowledgements

H. Derluyn holds a postdoctoral fellowship from the Research Foundation – Flanders (FWO) and acknowledges its support. The work reported in this paper has been supported by the KISADAMA project, funded by JPI Cultural Heritage within the Joint Heritage European Programme JHEP and by BOF research fund 01B00512 entitled 'Systems for controlling temperature and relative humidity' and by FWO research grant 1521815N. The Special Research Fund (BOF) of the Ghent University is acknowledged for the post-doctoral grant of M.N. Boone.

References

Boone, M.A., De Kock T., Bultreys T., De Schutter G., Vontobel P., Van Hoorebeke L. & Cnudde V. (2014). 3D mapping of water in oolithic limestone at atmospheric and vacuum saturation using X-ray micro-CT differential imaging. ***Materials Characterization*** 97: 150-160.

Desarnaud J., Derluyn H., Molari L., de Miranda S., Cnudde V. & Shahidzadeh N. (2015). Drying of salt contaminated porous media: effect of primary and secondary nucleation. ***Journal of Applied Physics***: under review.

Masschaele B., Dierick M., Van Loo D., Boone M.N., Brabant L., Pauwels E., Cnudde V. & Van Hoorebeke L. (2013). HECTOR: A 240kV micro-CT setup optimized for research. ***Journal of Physics: Conference Series*** 463: 012012.

Shahidzadeh-Bonn N., Desarnaud J., Bertrand F., Chateau X. & Bonn D. (2010). Damage in porous media due to salt crystallization. ***Physical Review E*** 81: 066110.

Vlassenbroeck J., Dierick M., Masschaele B., Cnudde V., Van Hoorebeke L. & Jacobs P. (2007). Software tools for quantification of X-ray microtomography. ***Nuclear Instruments & Methods In Physics Research Section A-Accelerators Spectrometers Detectors And Associated Equipment*** 580: 442-445.